photonics

MDPI

Article

Carbon Dot-Decorated Polystyrene Microspheres for Whispering-Gallery Mode Biosensing

Anton A. Starovoytov [1,*], Evgeniia O. Soloveva [1], Kamilla Kurassova [1], Kirill V. Bogdanov [1], Irina A. Arefina [1], Natalia N. Shevchenko [2], Tigran A. Vartanyan [1,*], Daler R. Dadadzhanov [1,*] and Nikita A. Toropov [1,3]

1 International Research and Education Center for Physics of Nanostructures, ITMO University, 49 Kronverksky Pr., St. Petersburg 197101, Russia; eugeniasoloveva11@gmail.com (E.O.S.); camillka713@gmail.com (K.K.); kirw.bog@gmail.com (K.V.B.); irina-arefina97@mail.ru (I.A.A.); n.a.toropov@soton.ac.uk (N.A.T.)
2 Institute of Macromolecular Compounds, Russian Academy of Sciences, St. Petersburg 199004, Russia; natali.shevchenko29@gmail.com
3 Optoelectronics Research Centre, University of Southampton, Southampton SO17 1BJ, UK
* Correspondence: anton.starovoytov@gmail.com (A.A.S.); tigran.vartanyan@mail.ru (T.A.V.); daler.dadadzhanov@gmail.com (D.R.D.)

Abstract: Whispering gallery mode (WGM) resonators doped with fluorescent materials find impressive applications in biological sensing. They do not require special conditions for the excitation of WGM inside that provide the basis for in vivo sensing. Currently, the problem of materials for in vivo WGM sensors are substantial since their fluorescence should have stable optical properties as well as they should be biocompatible. To address this we present WGM microresonators of 5–7 μm, where the dopant is made of carbon quantum dots (CDs). CDs are biocompatible since they are produced from carbon and demonstrate bright optical emission, which shows different bands depending on the excitation wavelength. The WGM sensors developed here were tested as label-free biosensors by detecting bovine serum albumin molecules. The results showed WGM frequency shifting, with the limit of detection down to 10^{-16} M level.

Keywords: whispering gallery modes; microsphere; carbon dots; biosensing; bovine serum albumin

Citation: Starovoytov, A.A.; Soloveva, E.O.; Kurassova, K.; Bogdanov, K.V.; Arefina, I.A.; Shevchenko, N.N.; Vartanyan, T.A.; Dadadzhanov, D.R.; Toropov, N.A. Carbon Dot-Decorated Polystyrene Microspheres for Whispering-Gallery Mode Biosensing. *Photonics* **2024**, *11*, 480. https://doi.org/10.3390/photonics11050480

Received: 20 April 2024
Revised: 9 May 2024
Accepted: 10 May 2024
Published: 20 May 2024

1. Introduction

In biological research and clinical diagnosis, it is crucial to detect and identify various proteins accurately. This process requires highly sensitive and selective detection methods. Many modern methods, which are well-developed, provide information about large ensembles of molecules and structures; however, sometimes it is required to detect unlabelled single proteins. Doped microresonators supporting whispering gallery modes (WGM) have gained attention as biosensors due to their biocompatibility, compact size, high Q-factor, and narrow spectral width of resonance lines [1,2]. They represent a logical way of further advancing WGM sensors and WGM-based optoplasmonic sensors, which are capable of detecting not just single molecules but also single atomic ions [3,4], tracking molecular movements during biochemical reactions [2], and collecting information about the spectral properties of molecules [5,6]. It is relatively easy to achieve lasing in such resonators [7]; however, biosensors based on WGM microlasers have been the focus for researchers for the last 10–15 years. Similarly to WGM sensors, WGM fluorescent sensors are highly responsive to even the slightest changes in the refractive index of the environment. This sensitivity enables the detection of frequency shifts caused by attaching molecules as it is in WGM sensors; while in WGM fluorescent sensors the number of detecting parameters can be extended. WGM fluorescent sensors have a wide range of applications, from the label-free detection of proteins and enzymes [2,8] to imaging in biological tissue [9]. In

addition, WGM-based sensors can be used to study drug interactions [10] and sensing at the cellular level [11], where WGM sensors embed in or interact with cells, enabling new applications for the in vivo sensing and tracking of physiological parameters of individual cells [12]. The sensitivity of WGM devices, coupled with their structural diversity and compatibility with existing infrastructures such as traditional chip-based technologies has led to the development of a wide range of sensor applications based on them.

Quantum dots are a popular choice for fluorescent dopants in the development of emitting WGM cavities. However, their use in biomedical applications may be limited due to potential toxicity issues arising from their composition of heavy metals. A non-toxic alternative to quantum dots is carbon dots (CDs), which are quasi-spherical nanoparticles less than 10 nm in size consisting of sp^2- or sp^3-carbon domains and rich in oxygen- and nitrogen-containing functional groups [13]. CDs are characterized by high biocompatibility, chemical inertness, photostability, and high photoluminescence quantum yield, which makes them most suitable for use in biological applications [14–16]. Carbon dots are water-soluble and have low toxicity, making them suitable for various medical applications, such as biosensing, drug delivery, and cell analysis [17,18]. When embedded into polystyrene microspheres, the carbon dots retain their biocompatibility. In our previous work on carbon dots, utilizing LIVE/DEAD and AlamarBlue assays we demonstrated the high biocompatibility of CDs on cell lines THP-1 (monocytes isolated from human peripheral blood), B16–F10 (mouse skin melanoma epithelial cell line), and K562 (human myelogenous leukemia cell line) [19]. CDs have been used as a gain medium for WGM lasers where the WGM resonator was made of conventional glass fiber [20]; the cavity sizes were up to 70 µm, which is barely suitable for in vivo biosensing. One of the first demonstrations of WGM lasers with CDs was made with CDs incorporated in NaCl; the Q-factor of such lasers was rather low—447 [21]. Recently, our group demonstrated a microfluidic approach to WGM cavities fabrication for another type of nanocrystals—AIS quantum dots [22]. Although a significant reduction in the emission lifetime was observed, there were no WGM resonances detected. Polystyrene microparticles decorated with CDs were used in [23], where their enhanced luminescence was observed. Although carbon dots are promising for biosensing and bioimaging [18], there are no reports about their use for WGM biosensors yet. So, in contrast to previously published works, here we focus on making WGM decorated with CDs for biosensing applications.

In this work, we present new composite WGM fluorescent sensors made of carbon quantum dots and polystyrene microspheres. We tested their sensing properties by applying bovine serum albumin (BSA) molecules—a protein that is commonly utilized as a reference protein for examining interactions with drugs, biomolecules, and nanoparticles. Its structural similarity to human serum albumin makes it a valuable tool for research in drug development and medical diagnostics [24,25]. Sensitive detection of BSA is crucial in a variety of applications; in biomedicine, BSA is used as a stabilizer of enzymes and proteins [26,27]; in pharmaceuticals, BSA is used as a drug carrier [28,29] due to its ability to bind and transport various compounds. Among numerous biomolecule detection methods, carbon-dot-doped WGM-based sensors offer a highly relevant approach for BSA protein detection. Their high sensitivity, ease of fabrication, low cost, biocompatibility, and selectivity make them valuable tools for various biomedical and analytical applications.

2. Materials and Methods

2.1. Synthesis of CDs

Multicolored carbon dots were synthesized by the solvothermal method described in [14], from citric acid and urea in dimethylformamide. Chemicals were sourced from reputable suppliers such as Sigma-Aldrich and LCC Vekton. To synthesize CDs, 1 g of citric acid and 2 g of urea were dissolved in 10 mL of dimethylformamide and heated in a Teflon-lined autoclave at 180 °C for 8 h. The colloidal solution obtained was purified by dialysis against deionized water using a dialysis tube with a 3.5 kDa molecular cut-off tube for 24 h and then freeze-dried.

2.2. Synthesis of Polystyrene Microspheres

Polystyrene microspheres with diameters ranging from 5 to 7 μm were synthesized via emulsifier-free emulsion and dispersion copolymerization using a combination of styrene and 4-styrenesulfonic acid sodium salt (NaSS) [30,31]. Styrene was purified using a 30% aqueous solution of potassium hydroxide followed by distillation under vacuum. Emulsifiers including sodium dodecyl sulfate, Tween 80, Tween 65, dioctyl sulfosuccinate sodium salt, and poly(vinyl alcohol) were used without prior purification. Bidistilled water, free from surface active impurities as indicated by specific conductivity and surface tension measurements, was utilized for solution preparation and polymerization. The synthesis was conducted in a 100 mL flask equipped with standard laboratory apparatuses for temperature control and agitation. A mixture of styrene and NaSS in appropriate solvents was heated to specified temperatures to initiate polymerization. After completion, the residual monomer was removed by steam distillation, and water-soluble impurities were eliminated through centrifugation and redispersion cycles.

2.3. Impregnation of CDs into Microspheres

To decorate microspheres with CDs, we adopted the impregnation method. This method was selected due to its cost-effectiveness and simplicity, making it an attractive choice for modifying the properties of loose polymeric and mesoporous materials [32,33]. Impregnation involves saturating the microspheres with a solution containing carbon dots, allowing for their uniform distribution throughout the microsphere matrix without compromising their structural integrity. To 100 μL of an aqueous solution with a 10^{-3} M concentration of CDs, 600 μL of an aqueous solution of polystyrene particles (0.5 wt%) was added, with the resulting solution occasionally shaken over 20 h. It was then washed with deionized water after which the solution was centrifuged three times for 10 min at 5000× *g*. Upon aggregation of the microspheres, the solution was held in an ultrasonic bath until the particles dissolved completely in water (1–2 min).

2.4. WGM Sensing

To study the sensor properties of CD-decorated microspheres supporting WGM in relation to the presence of BSA, they were deposited from an aqueous buffer onto a glass substrate and subsequently dried under ambient conditions. Preliminary CD concentration in the aqueous buffer was reduced to ensure that any droplet of the solution contains from two to five microspheres. The stock solution of BSA with a concentration of $1.5 \cdot 10^{-5}$ M was prepared by dissolving 10 mg powder in 10 mL of distilled water. Then, a range of BSA solutions with concentrations from 10^{-12} to 10^{-18} M were prepared by dilution of the stock solution. During the experiment, the BSA solution was added to the same slide where polystyrene microspheres with CDs were already deposited and the same particles were examined for changes in their emission.

2.5. Characterization

To measure the absorption spectra of solutions over a wide spectral range with a step of 1 nm, a spectrophotometer SF-56 (St. Petersburg, Russia) was used; luminescence spectra were measured using a spectrofluorometer Shimadzu RF-5301PC (Kyoto, Japan). The laser scanning confocal microscope Zeiss LSM 710 (Jena, Germany) was used to obtain luminescent images of microspheres doped with CDs. An objective 20×/0.4 was selected to study the samples with excitation wavelengths of 405 and 488 nm. To detect emission and whispering gallery modes, a confocal Raman microspectrometer inVia Renishaw (New Mills, UK) was used, with sample emission excited by a laser with a wavelength of 488 nm. A microscopic image of microspheres was obtained by scanning electron microscope (SEM) Merlin (Zeiss).

3. Results and Discussion

The absorption spectrum of CDs in water (Figure 1) shows two distinct bands. The short-wavelength band in the ultraviolet region represents a combination of transitions involving π–π^* transitions in the sp^2-hybridized carbon core and n–π^* transitions of carboxyl groups [14,34,35]. The absorption peak at 535 nm corresponds to the transitions related to the surface states. Given BSA's limited absorption in the visible spectrum, the optical behavior of the mixture solution of BSA and CDs primarily reflects the inherent properties of carbon dots.

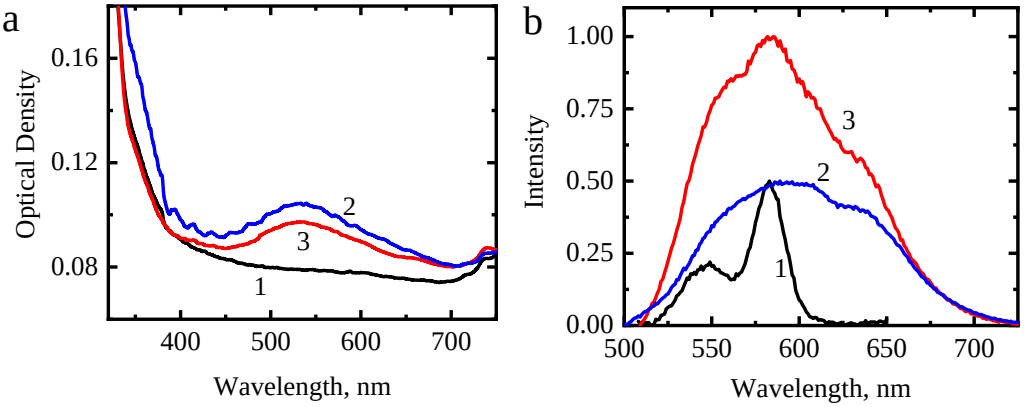

Figure 1. Spectra of water solutions: optical density (**a**) and normalized photoluminescence (**b**) of BSA (1), CDs (2), and their mixture excited at λ = 488 nm (3).

CDs exhibit predominant photoluminescence in the mixture's spectra (Figure 1b), overshadowing the luminescent bands of bovine serum albumin. These bands, with peaks at 548 nm and 583 nm, are only faintly discernible. The fluorescence spectrum of carbon dots changes when they are embedded into polymer microspheres (Figure 2a) from the solution, which is explained by characteristic mechanisms such as surface passivation, aggregation effects, confinement effects, charge transfer, and/or polarity changes (Figure 2b) [36–39]. Meanwhile, the fluorescence spectra of CDs exhibit excitation-dependent emission due to the coexistence of multiple emissive centers within carbon dots.

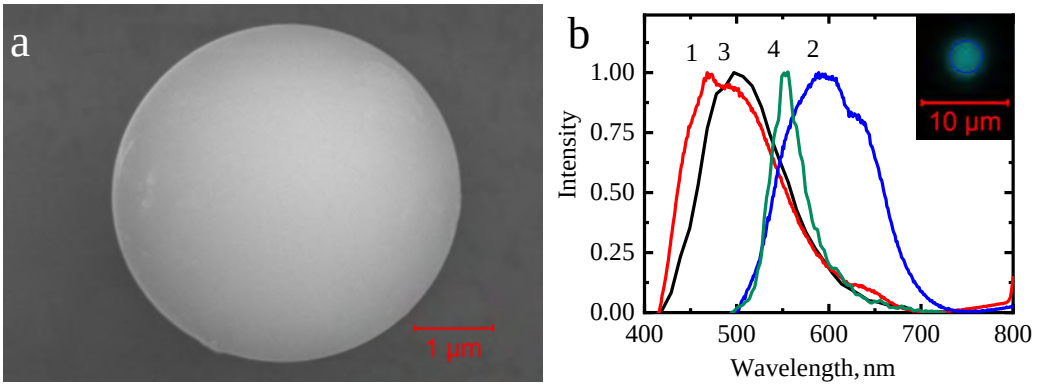

Figure 2. (**a**) SEM image of a polystyrene microsphere. (**b**) Normalized photoluminescence spectra of CDs solution excited at 405 nm (curve 1) and 488 nm (curve 2), CD-doped microspheres excited at 405 nm (curve 3) and 488 nm (curve 4). Inset shows a microsphere image, corresponding to spectrum 3, which was acquired by a laser scanning confocal microscope.

The emission spectra of the obtained microspheres were measured with the micro-Raman spectrometer inVia, with 50 pm resolution (Figure 3a). They have two peculiarities. First, the emission spectra of CDs doped microspheres have similar bands to the solution of CDs (Figure 2b); however, we observe emission peaks corresponding to the whispering-

gallery modes circulating inside the microsphere. This is the result of coupling between CD emission and cavity modes and amplified spontaneous emission. To check for possible lasing, an input–output characteristic was measured at different excitation levels. Figure 3b shows that the peak intensities are sublinear, with the characteristic saturation, corresponding to typical quantum dots [40].

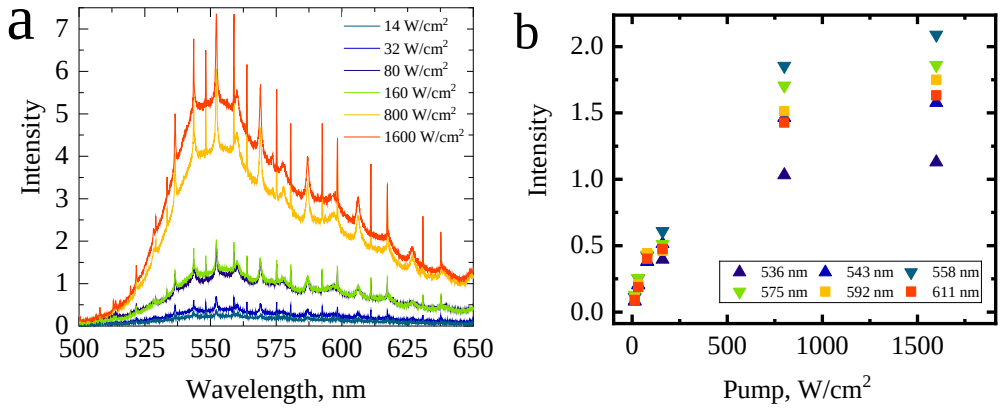

Figure 3. (**a**) Emission spectra of polystyrene microspheres covered with carbon dots at different excitation intensities; (**b**) input-output characteristic defined as intensities of separate emission lines.

For sensing experiments, 4 µL of the aqueous BSA solution was added to the test sample; a concentration series of experiments with BSA (10^{-12} M, 10^{-15} M, 10^{-16} M, 10^{-18} M) was conducted to determine the limit of detection, that is reflected on Figure 4. The mode shifting is caused by changing the surrounding medium refractive index, so-called reactive sensing [5]. Note, that wavelength shifts values are huge; even for 10^{-15} M it is about 1.5 nm (Figure 4b), and it became smaller with a reduced concentration of BSA (Figure 4c). The second feature we observed is related to reducing the Q-factor of the resonances under the attachment of BSA molecules, which is also related to sensing [41]. This is because the adsorption of molecules on the surface of the resonator can increase the energy dissipated by the resonator, leading to a lower Q-factor. Indeed, as seen in Figure 4a, the value of Q-factors is changing; according to our assessments, it was reduced from 2820 to 1650 on average (please see Appendix A). However, the Q-factor is still high enough for observing amplified emission.

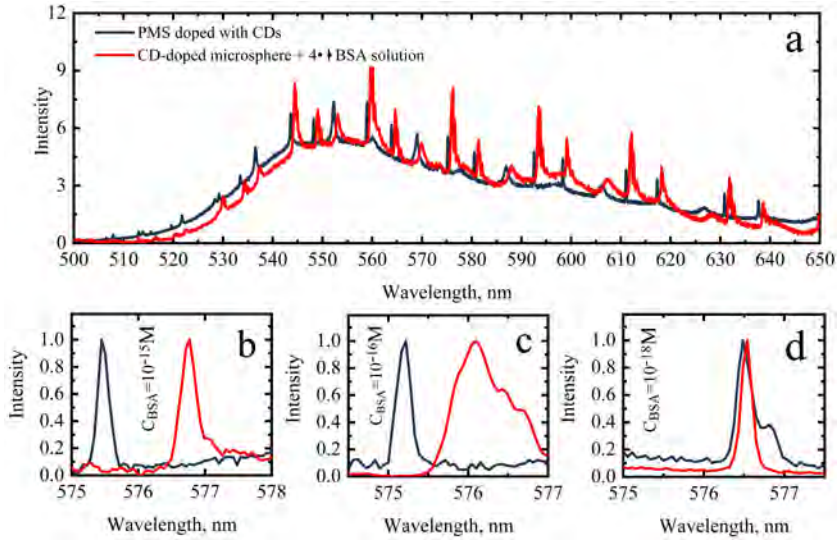

Figure 4. (**a**) Emission spectra of CDs doped microspheres before and after adding BSA molecules (10^{-16} M solution). WGM frequency shift extracted from emission spectra of CDs doped microspheres before and after adding BSA solution: (**b**)—10^{-15} M, (**c**)—10^{-16} M, (**d**)—10^{-18} M.

As a further step, we tried to find a limit of detection. For this, the resulting BSA concentration was reduced to 10^{-18} M and applied to samples of CDs doped WGM microspheres. The results are presented in Figure 4d. The normalized spectra show the reproducible character of frequency shifts; however, at 10^{-18} M it is becoming unresolvable with our sensors. Thus, we define the limit of detection as 10^{-16} M and the dynamic range as four orders of magnitude of concentrations at least (Figure 5).

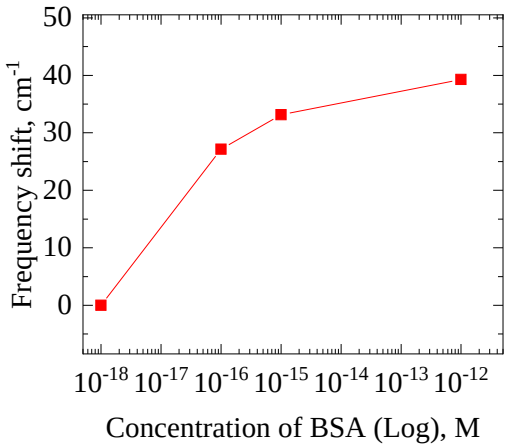

Figure 5. Dependence of WGM frequency shift vs. concentration of added BSA solution in logarithmic scale.

4. Conclusions

We have developed a simple and reproducible method for making biosensors based on fluorescent whispering gallery mode resonators. This method exploits the decorating of polystyrene microspheres with carbon quantum dots. Such particles demonstrate narrow emission lines corresponding to whispering gallery modes. The method allows the production of particles for label-free sensing of low concentrations of biomolecules such as bovine serum albumin by WGM frequency shifting. The detection limit is defined as low as 10^{-16} M concentrations and the dynamic range is four orders of magnitude.

Author Contributions: Conceptualization, N.A.T.; investigation, A.A.S., E.O.S., K.K., K.V.B., I.A.A. and N.N.S.; writing—original draft preparation, A.A.S., E.O.S. and K.K.; writing—review and editing, A.A.S., E.O.S., K.K., D.R.D. and T.A.V.; visualization, A.A.S., E.O.S. and K.K.; supervision, A.A.S.; project administration, A.A.S. and D.R.D.; funding acquisition, D.R.D. All authors have read and agreed to the published version of the manuscript.

Funding: This work was supported by the Russian Science Foundation (Project 22-72-10057).

Institutional Review Board Statement: The study did not require ethical approval.

Informed Consent Statement: Not applicable.

Data Availability Statement: The authors confirm that the data supporting the findings of this study are available within the article.

Acknowledgments: The authors acknowledge Mikhail. A. Baranov for providing the SEM-image of the polystyrene microparticles and Sofia A. Khorkina for the Raman spectra measurements.

Conflicts of Interest: The authors declare no conflicts of interest. N.A.T. is currently with the University of Southampton. He provided his consent for the publication.

Abbreviations

The following abbreviations are used in this manuscript:

CDs	Carbon dots
WGM	Whispering gallery mode
BSA	Bovine serum albumin

Appendix A

Table A1 presents the spectral position of WGM modes, the full width at half maximum (FWHM), and the corresponding Q-factors of the carbon dot (CD)-doped microspheres before and after the addition of bovine serum albumin (BSA) solution at various concentrations. The observed trend of decreasing Q-factors in CD-doped microspheres following the addition of BSA solution is attributed to the adsorption of protein biomolecules onto the microsphere surface, which can lead to increased energy dissipation.

Table A1. WGM modes characteristics of CDs-doped microspheres before and after covering by BSA.

Sample	Peak	λ, nm	FWHM, nm	Q-Factor
1. CD-doped Microsphere	1	561.54	0.289	1954 ± 100
	2	577.89	0.312	1863 ± 96
	3	595.28	0.350	1711 ± 91
1. CD-doped microsphere after adding BSA solution (10^{-12} M)	1	564.77	0.375	1497 ± 78
	2	581.21	0.405	1427 ± 74
	3	598.76	0.365	1631 ± 85
2. CD-doped microsphere	1	559.18	0.224	2496 ± 170
	2	575.45	0.205	2807 ± 184
	3	592.82	0.2	2963 ± 194
2. CD-doped microsphere after adding BSA solution (10^{-15} M)	1	560.45	0.318	1762 ± 150
	2	576.77	0.290	1989 ± 154
	3	594.14	0.273	2176 ± 169
3. CD-doped microsphere	1	558.95	0.211	2649 ± 80
	2	575.22	0.214	2688 ± 82
	3	592.54	0.208	2849 ± 86
3. CD-doped microsphere after adding BSA solution (10^{-16} M)	1	559.87	0.415	1349 ± 140
	2	576.26	0.324	1779 ± 176
	3	593.47	0.388	1530 ± 150

References

1. Toropov, N.; Cabello, G.; Serrano, M.P.; Gutha, R.R.; Rafti, M.; Vollmer, F. Review of biosensing with whispering-gallery mode lasers. *Light Sci. Appl.* **2021**, *10*, 42 . [CrossRef] [PubMed]
2. Houghton, M.C.; Kashanian, S.V.; Derrien, T.L.; Masuda, K.; Vollmer, F. Whispering-Gallery Mode Optoplasmonic Microcavities: From Advanced Single-Molecule Sensors and Microlasers to Applications in Synthetic Biology. *ACS Photonics* **2024**, *11*, 892–903. [CrossRef] [PubMed]
3. Baaske, M.D.; Vollmer, F. Optical observation of single atomic ions interacting with plasmonic nanorods in aqueous solution. *Nat. Photonics* **2016**, *10*, 733–739. [CrossRef]
4. Duan, R.; Li, Y.; Li, H.; Yang, J. Detection of heavy metal ions using whispering gallery mode lasing in functionalized liquid crystal microdroplets. *Biomed. Opt. Express* **2019**, *10*, 6073–6083. [CrossRef] [PubMed]
5. Toropov, N.A.; Houghton, M.C.; Yu, D.; Vollmer, F. Thermo-optoplasmonic single-molecule sensing on optical microcavities. *bioRxiv* **2023**. [CrossRef]
6. Yu, X.C.; Tang, S.J.; Liu, W.; Xu, Y.; Gong, Q.; Chen, Y.L.; Xiao, Y.F. Single-molecule optofluidic microsensor with interface whispering gallery modes. *Proc. Natl. Acad. Sci. USA* **2022**, *119*, e2108678119. [CrossRef] [PubMed]
7. Garrett, C.G.B.; Kaiser, W.; Bond, W.L. Stimulated Emission into Optical Whispering Modes of Spheres. *Phys. Rev.* **1961**, *124*, 1807–1809. [CrossRef]
8. Wang, H.; Xu, T.; Xu, T.; Wang, Z.; Wang, Z.; Liu, Y.; Chen, H.; Jiang, J.; Jiang, J.; Liu, T. Highly sensitive and label-free detection of biotin using a liquid crystal-based optofluidic biosensor. *Biomed. Opt. Express* **2023**, *14*, 3763–3774. [CrossRef] [PubMed]

9. Li, X.; Qin, Y.; Tan, X.; Chen, Y.C.; Chen, Q.; Weng, W.H.; Wang, X.; Fan, X. Ultrasound Modulated Droplet Lasers. *ACS Photonics* **2019**, *6*, 531–537. [CrossRef]
10. Álvarez Freile, J.; Choukrani, G.; Zimmermann, K.; Bremer, E.; Dähne, L. Whispering Gallery Modes-based biosensors for real-time monitoring and binding characterization of antibody-based cancer immunotherapeutics. *Sens. Actuators B* **2021**, *346*, 130512. [CrossRef]
11. Karl, M.; Dietrich, C.P.; Schubert, M.; Samuel, I.D.W.; Turnbull, G.A.; Gather, M.C. Single cell induced optical confinement in biological lasers. *J. Phys. D Appl. Phys.* **2017**, *50*, 084005. [CrossRef]
12. Schubert, M.; Woolfson, L.; Barnard, I.R.M.; Dorward, A.M.; Casement, B.; Morton, A.; Robertson, G.B.; Appleton, P.L.; Miles, G.B.; Tucker, C.S.; et al. Monitoring contractility in cardiac tissue with cellular resolution using biointegrated microlasers. *Nat. Photonics* **2020**, *14*, 452–458. [CrossRef]
13. Stepanidenko, E.A.; Ushakova, E.V.; Fedorov, A.V.; Rogach, A.L. Applications of Carbon Dots in Optoelectronics. *Nanomaterials* **2021**, *11*, 364. [CrossRef] [PubMed]
14. Döring, A.; Ushakova, E.; Rogach, A.L. Chiral carbon dots: Synthesis, optical properties, and emerging applications. *Light Sci. Appl.* **2022**, *11*, 75 . [CrossRef] [PubMed]
15. Jing, H.H.; Bardakci, F.; Akgöl, S.; Kusat, K.; Adnan, M.; Alam, M.J.; Gupta, R.; Sahreen, S.; Chen, Y.; Gopinath, S.C.B.; et al. Green Carbon Dots: Synthesis, Characterization, Properties and Biomedical Applications. *J. Funct. Biomater.* **2023**, *14*, 27. [CrossRef] [PubMed]
16. Sahu, S.; Behera, B.; Maiti, T.K.; Mohapatra, S. Simple one-step synthesis of highly luminescent carbon dots from orange juice: Application as excellent bio-imaging agents. *Chem. Commun.* **2012**, *48*, 8835–8837. [CrossRef] [PubMed]
17. Ji, C.; Zhou, Y.; Leblanc, R.M.; Peng, Z. Recent Developments of Carbon Dots in Biosensing: A Review. *ACS Sens.* **2020**, *5*, 2724–2741. [CrossRef]
18. Wang, B.; Cai, H.; Waterhouse, G.I.N.; Qu, X.; Yang, B.; Lu, S. Carbon Dots in Bioimaging, Biosensing and Therapeutics: A Comprehensive Review. *Small Sci.* **2022**, *2*, 2200012. [CrossRef]
19. Vedernikova, A.A.; Miruschenko, M.D.; Arefina, I.A.; Xie, J.; Huang, H.; Koroleva, A.V.; Zhizhin, E.V.; Cherevkov, S.A.; Timin, A.S.; Mitusova, K.A.; et al. Green and Red Emissive N,O-Doped Chiral Carbon Dots Functionalized with l-Cysteine. *J. Phys. Chem. Lett.* **2024**, *15*, 113–120. [CrossRef]
20. Han, Z.; Ni, Y.; Ren, J.; Zhang, W.; Wang, Y.; Xie, Z.; Zhou, S.; Yu, S.F. Highly efficient and ultra-narrow bandwidth orange emissive carbon dots for microcavity lasers. *Nanoscale* **2019**, *11*, 11577–11583. [CrossRef]
21. Liu, H.; Wang, F.; Wang, Y.; Mei, J.; Zhao, D. Whispering Gallery Mode Laser from Carbon Dot–NaCl Hybrid Crystals. *ACS Appl. Mater. Interfaces* **2017**, *9*, 18248–18253. [CrossRef] [PubMed]
22. Kurassova, K.; Filatov, N.A.; Alexan, G.; Dadadzhanova, A.I.; Dadadzhanov, D.R.; Toropov, N.A.; Vartanyan, T.A. Microfluidic Fabrication of Polymeric Microspheres Doped with Quantum Dots for Biosensors. In *Optical Sensors: Proceedings Optica Sensing Congress 2023, AIS, FTS, HISE, Sensors, ES 2023*; Optica Publishing Group: Washington, DC, USA, 2023. [CrossRef]
23. Venkatakrishnarao, D.; Sahoo, C.; Vattikunta, R.; Annadhasan, M.; Naraharisetty, S.R.G.; Chandrasekar, R. 2D Arrangement of Polymer Microsphere Photonic Cavities Doped with Novel N-Rich Carbon Quantum Dots Display Enhanced One- and Two-Photon Luminescence Driven by Optical Resonances. *Adv. Opt. Mater.* **2017**, *5*, 1700695. [CrossRef]
24. Jahanban-Esfahlan, A.; Ostadrahimi, A.; Jahanban-Esfahlan, R.; Roufegarinejad, L.; Tabibiazar, M.; Amarowicz, R. Recent developments in the detection of bovine serum albumin. *Int. J. Biol. Macromol.* **2019**, *138*, 602–617. [CrossRef] [PubMed]
25. Adamczyk, O.; Szota, M.; Rakowski, K.; Prochownik, M.; Doveiko, D.; Chen, Y.; Jachimska, B. Bovine Serum Albumin as a Platform for Designing Biologically Active Nanocarriers—Experimental and Computational Studies. *Int. J. Mol. Sci.* **2023**, *25*, 37. [CrossRef] [PubMed]
26. Duskey, J.T.; da Ros, F.; Ottonelli, I.; Zambelli, B.; Vandelli, M.A.; Tosi, G.; Ruozi, B. Enzyme Stability in Nanoparticle Preparations Part 1: Bovine Serum Albumin Improves Enzyme Function. *Molecules* **2020**, *25*, 4593. [CrossRef] [PubMed]
27. Mafra, A.C.O.; Kopp, W.; Beltrame, M.B.; de Lima Camargo Giordano, R.; de Arruda Ribeiro, M.P.; Tardioli, P.W. Diffusion effects of bovine serum albumin on cross-linked aggregates of catalase. *J. Mol. Catal. B Enzym.* **2016**, *133*, 107–116. [CrossRef]
28. Mardikasari, S.A.; Katona, G.; Sipos, B.; Ambrus, R.; Csóka, I. Preparation and Optimization of Bovine Serum Albumin Nanoparticles as a Promising Gelling System for Enhanced Nasal Drug Administration. *Gels* **2023**, *9*, 896. [CrossRef] [PubMed]
29. Ma, N.; Liu, J.; He, W.; Li, Z.; Luan, Y.; Song, Y.; Garg, S. Folic acid-grafted bovine serum albumin decorated graphene oxide: An efficient drug carrier for targeted cancer therapy. *J. Colloid Interface Sci.* **2017**, *490*, 598–607. [CrossRef] [PubMed]
30. Shevchenko, N.; Tomšík, E.; Laishevkina, S.; Iakobson, O.; Pankova, G. Cross-linked polyelectrolyte microspheres: Preparation and new insights into electro-surface properties. *Soft Matter* **2021**, *17*, 2290–2301. [CrossRef]
31. Laishevkina, S.; Iakobson, O.; Saprykina, N.; Dobrodumov, A.; Chelibanov, V.; Tomšík, E.; Shevchenko, N. Hydrophilic polyelectrolyte microspheres as a template for poly(3,4-ethylenedioxythiophene) synthesis. *Soft Matter* **2023**, *19*, 4144–4154. [CrossRef]
32. Song, S.A.; Jung, K.Y.; Oh, J.Y.; Chang, Y.W.; Kim, K.; Lim, S.N.; Jeong, Y.C. Enhancement of cell performance using nano polystyrene beads in photoelectrodes for dye-sensitized solar cells. *J. Taiwan Inst. Chem. Eng.* **2017**, *78*, 195–199. [CrossRef]
33. Nabiullina, R.D.; Nikitin, I.Y.; Soloveva, E.O.; Gladskikh, I.A.; Starovoytov, A.A. Optical properties of nanoporous aluminum oxide activated by molecular clusters of pseudoisocyanine dye. In *Proceedings of SPIE, Nanophotonics IX*; SPIE: Bellingham, WA, USA , 2022; Volume 12131, pp. 170–174. [CrossRef]

34. Đorđević, L.; Arcudi, F.; D'Urso, A.; Cacioppo, M.; Micali, N.; Bürgi, T.; Purrello, R.; Prato, M. Design principles of chiral carbon nanodots help convey chirality from molecular to nanoscale level. *Nat. Commun.* **2018**, *9*, 3442 . [CrossRef]
35. Li, F.; Li, Y.; Yang, X.; Han, X.; Jiao, Y.; Wei, T.; Yang, D.; Xu, H.; Nie, G. Highly Fluorescent Chiral N-S-Doped Carbon Dots from Cysteine: Affecting Cellular Energy Metabolism. *Angew. Chem. Int. Ed.* **2018**, *57*, 2377–2382. [CrossRef] [PubMed]
36. Vedernikova, A.A.; Miruschenko, M.D.; Arefina, I.A.; Babaev, A.A.; Stepanidenko, E.A.; Cherevkov, S.A.; Spiridonov, I.G.; Danilov, D.V.; Koroleva, A.V.; Zhizhin, E.V.; et al. Dual-Purpose Sensing Nanoprobe Based on Carbon Dots from o-Phenylenediamine: PH and Solvent Polarity Measurement. *Nanomaterials* **2022**, *12*, 3314. [CrossRef] [PubMed]
37. Zulfajri, M.; Sudewi, S.; Ismulyati, S.; Rasool, A.; Adlim, M.; Huang, G.G. Carbon Dot/Polymer Composites with Various Precursors and Their Sensing Applications: A Review. *Coatings* **2021**, *11*, 1100. [CrossRef]
38. Kar, D.K.; Praveenkumar, V.; Si, S.; Panigrahi, H.; Mishra, S. Carbon Dots and Their Polymeric Nanocomposites: Insight into Their Synthesis, Photoluminescence Mechanisms, and Recent Trends in Sensing Applications. *ACS Omega* **2024**, *9*, 11050–11080. [CrossRef]
39. Mohammad-Jafarieh, P.; Akbarzadeh, A.; Salamat-Ahangari, R.; Pourhassan-Moghaddam, M.; Jamshidi-Ghaleh, K. Solvent effect on the absorption and emission spectra of carbon dots: Evaluation of ground and excited state dipole moment. *BMC Chem.* **2021**, *15*, 53. [CrossRef] [PubMed]
40. Foell, C.A.; Schelew, E.; Qiao, H.; Abel, K.A.; Hughes, S.; van Veggel, F.C.J.M.; Young, J.F. Saturation behaviour of colloidal PbSe quantum dot exciton emission coupled into silicon photonic circuits. *Opt. Express* **2012**, *20*, 10453–10469. [CrossRef]
41. Arnold, S.; Khoshsima, M.; Teraoka, I.; Holler, S.; Vollmer, F. Shift of whispering-gallery modes in microspheres by protein adsorption. *Opt. Lett.* **2003**, *28*, 272–274. [CrossRef]